Chemical Methodologies 4(2020) 477-493

Chemical Methodologies

Journal homepage: http://chemmethod.com

Original Research article

Preparation of Xanthan Magnetic Biocompatible Nano-Composite for Removal of Ni^2+ from Aqueous Solution

Alireza Bozorgian[a,*], Soroush Zarinabadi[b], Amir Samimi[a]

[a] Department of Chemical Engineering, Mahshahr Branch, Islamic Azad University, Mahshahr, Iran

[b] Department of Engineering, Ahvaz Branch, Islamic Azad University, Ahvaz, Iran

ARTICLE INFORMATION

Received: 02 January 2020
Received in revised: 23 January 2020
Accepted: 05 April 2020
Available online: 01 July 2020

DOI: 10.33945/SAMI/CHEMM.2020.4.9

KEYWORDS

Adsorption
Hydrogel adsorbent
Nickel
Nickel-xanthan removal

ABSTRACT

This study investigates the uptake of the nickel (II) metal ions from aqueous sources using the xanthan magnetic biocompatible nano-composites. The desired nano-sorbent was first synthesized, analysed, and evaluated by scanning electron microscope (SEM) and Fourier transform infrared spectroscopy and (FT-IR), then used as adsorbent for removing the nickel from aqueous solution. Then the effect of different parameters such as contact time, adsorbent amount, pH, initial concentration, and temperature on the adsorption rate was investigated. The equilibrium time for the stirring state was 60 min and the optimum adsorbent value was 0.1 g and the acidity of 4 was the best pH. The highest removal efficiency was obtained at 97.6%. The kinetic studies of nickel removal by the synthesized adsorbent were performed and the results obtained for batch experiments follow the pseudo-quadratic kinetic model with (R^2=0.9987). Equilibrium adsorption studies also revealed that, the adsorption process was in better agreement with the Freundlich isotherm (R^2=0.9978). The positive Gibbs free energy (15.08 KJ/mole^{-1}) showed that the process was spontaneous. Also the entropy changes was positive (0.03 KJ/mole^{-1}), indicated an increase in entropy during the adsorption process in the system. Therefore, the adsorption process was associated with increasing the disorder.

*Corresponding author: E-mail: a.bozorgian@mhriau.ac.ir, Department of Engineering, Department of Chemical Engineering, Mahshahr Branch, Islamic Azad University, Mahshahr, Iran, Tel: +989169206615

Graphical Abstract

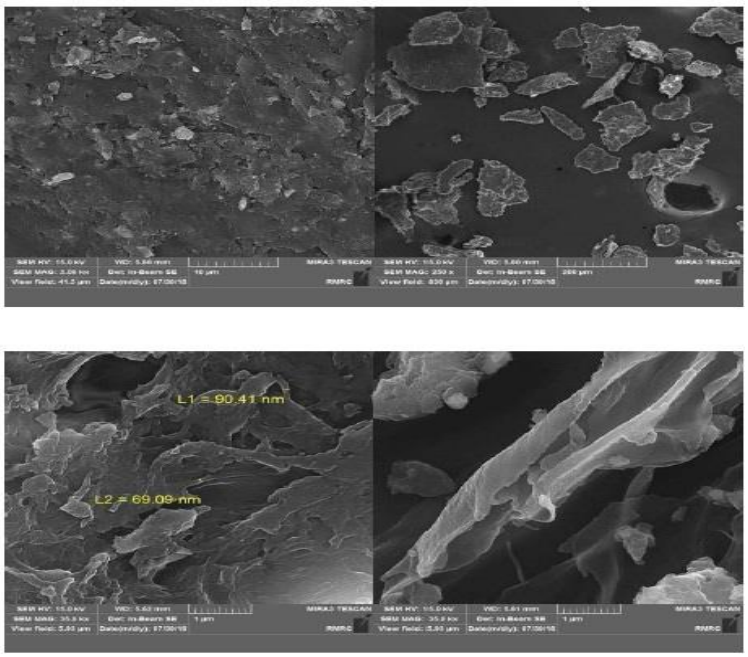

Introduction

With the advent of human civilization, by developing the technology and the ever-increasing population the world now face with a problem called pollution in air, soil and water. Water, as a compound that covers three-quarters of the entire surface of the earth, is one of the essential factors for the survival of all human, animal, and plant life [1-2]. In recent years, different methods have used to remove heavy metals from wastewater. These methods include ion exchange, coagulation, sedimentation, adsorption, and sedimentation/adsorption [3]. In 2018, Rodriguez *et al.,* investigated the adsorption of Ni (II) onto inexpensive activated carbon derived from spent coffee (SAC) and coffee husk (HAC) and measured the porous tissues of the adsorbents by measurements N_2 and CO_2 uptake were characterized [4-7]. They evaluated Ni (II) adsorption using different adsorption isotherm models (Langmuir and Freundlich) and determined their thermodynamics and kinetic parameters. Their results showed that, both the adsorbents had a high affinity for Ni (II); however, the surface area and size of the AC pores were not a determining factor in the adsorption process. These adsorbents have a micro porous nature. In contrast, the higher oxygen content associated with minerals such as K_2O and carbonic factors related with O-H in HAC for the Ni adsorption process are crucial. Thermodynamic parameters such as $\Delta G°$, $\Delta H°$, $\Delta S°$ confirmed that the adsorption process is spontaneous, random, and endothermic. In addition, the recoverable adsorption and adsorption of Aur-O and EBT from aqueous solution showed a decrease in

activity after six and three periods of use. Therefore, synthetic adsorbents can successfully use by the textile industry for the treatment of contaminated water [55]. Mital *et al.*, (2014) assessed the adsorption of the malachite green dye using xanthan magnetic hydrogels (Gx)/Fe_3O_4. The hydrogel nano-composite Gx-cl-P (AA-coAAm)/Fe_3O_4 was fabricated by combining the magnetic nanoparticles Fe_3O_4 in the polymer matrix of xanthan hydrogel with polymeric composition. The maximum adsorption observed in neutral pH solution with 0.2 g/L nano-composite Gx-cl-P (AA-coAAm)/Fe_3O_4. The adsorbed isotherm data were presented using five isotherm models such as Langmuir, Freundlich, Temkin, Flori-Hoggins isotherm models, and the adsorption process was followed by Langmuir isotherm model with maximum adsorption capacity of 497.15 mg/g. Adsorption-desorption studies demonstrated that the hydrogel nano-composite Gx-cl-P (AA-coAAm)/Fe_3O_4 can be repeatedly used for MG adsorption [8-10]. Nickel is an element with an atomic number of 28, the scientific symbol of Ni in group VII and is in the fourth period periodic table. It is in iron group that is hard and flexible, conductor of electricity and easily combined with sulfur and arsenic [11].

Experimental

Computation theory: Adsorption is a process in which atoms, ions or molecules of a gas, liquid, or solid bonded to a surface. The precise nature of this binding depends on the details of the species involved in the adsorption process. Surface adsorption occurs because of surface energy. In the adsorption process, a film of adsorbed material created on the adsorbent surface [12-15].

Table 1. Isotherm parameters for MG adsorption on Gx-cl-P (AA-coAAm)/Fe_3O_4 on hydrogel nano composite

Isotherms	Isotherm constants	25 °C	35 °C
Langmuir	$q_m(mg/g)$	497.512	512.82
	b	0.1694	0.2012
	R^2	0.999	0.999
	R_L	0.025-0.196	0.211-0.171
Freundlich	1/n	0.463	0.477
	K_F	83.708	92.31
	R^2	0.933	0.927
Temkin	β	0.0108	0.0101
	R^2	0.992	0.991
Flory-higgins	K_α	5.53e-4	4.43e-4
	$-\Delta G^\circ$ (kJ/mol)	18.566	19.611
	n	1.111	1.089
	R^2	0.898	0.858
Dubinin-kaganer-radushkevich (DVR)	$\beta \times 10^{-3}$	3.67	2.91
	q_D(mg/g)	310.44	326.35
	E(kJ/mol)	1.167	1.310
	R^2	0.778	0.796

Table 2. Kinetics parameters for MG adsorption on Gx-cl-P (AA-coAAm)/Fe_3O_4 hydrogel nano-composite

Kinetic model	Kinetic parameters	50 mg/L	75 mg/L	100 mg/L
Pseudo first order	$k_1 \times 10^{-3}$	112.8	20.35	20.86
	q_e(cal.)	68.54	59.202	99.77
	q_e(exp.)	81.202	101.86	194.20
	R^2	0.851	0.803	0.786
Pseudo second order	$k_2 \times 10^{-3}$	10.2	2.620	1.72
	q_e(cal.)	82.85	102.88	195.694
	q_e(exp.)	81.202	101.86	194.20
	R^2	0.999	0.999	0.999
Elovich	$\beta \times 10^{-2}$	13.30	4.171	2.71
	R^2	0.903	0.942	0.972
Liquid film diffusion	$K_{fd} \times 10^{-2}$	13.08	9.04	9.04
	R^2	0.869	0.880	0.896
Intra particle diffusion	K_i	19.221	21.145	38.498
	C_i	13.509	5.122	20.02
	R^2	0.846	0.947	0.933

Table 3. Langmuir isotherm parameters for MG adsorption on Gx-cl-P (AA-coAAm) / Fe_3O_4 hydrogel nano-composite

Isotherms	Isotherm constants		
	q_m (mg/g)	b(L/mg)	R^2
Langmuir	357.17	0.121	0.990

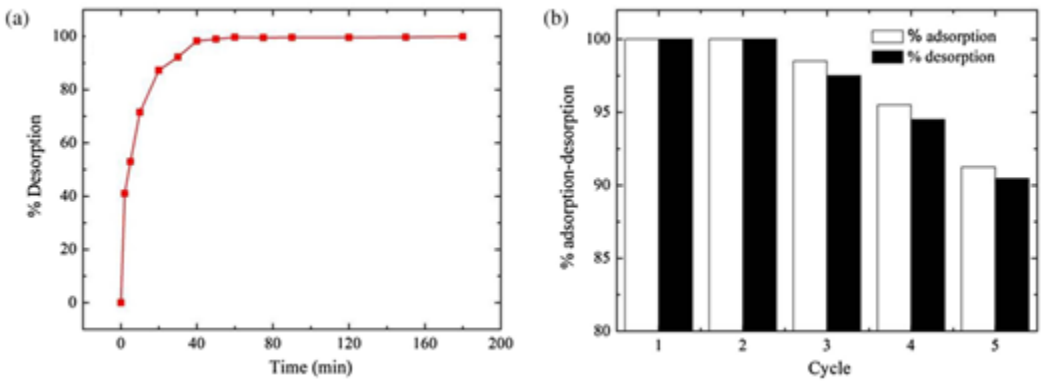

Figure 1. (a) MG adsorption kinetics of hydrogel composite Gx-cl-P (AA-coAAm)/Fe_3O_4 in acid solution HCl 0.1 M; (b) Performance of hydrogel nano composite Gx-cl-P (AA-coAAm)/Fe_3O_4 with several reconstruction periods

Required chemicals

All the chemicals utilized in this study purchased from Merck and Sigma Aldrich, Germany.

Table 4. Required chemicals for conduct research

g/mol	Symbol	Material
290.81	$NiN_2O_8*H_2O$	Nickel nitrate hexahydrate
36.5	HCl	Ric acid chloride
40	NaOH	Sodium hydroxide
63	HNO_3	Nitric acid
18	DM water	Distilled water
58.08	Acetone	Stan
231.53	MNP Fe_3O_4	Iron nanoparticles
Monomer	$C_{35}H_{49}O_{29}$	Xanthan
270.32	$K_2S_2O_8$	High potassium sulfate
154.17	$C_7H_{10}N_2O_2$	Methylene base acrylamide
72.06	$C_3H_4O_2$	Acrylic acid
71.08	C_3H_5NO	Acrylamide

Required machines

Spectrophotometer analysis (CARY100 machine made in US) was used to determine the concentration of nickel ions. pH meter (model 827, Switzerland) was utilized to measure and adjust the pH of the solutions. To disperse the iron nanoparticles, ultrasonic machine (model DK203 H, Germany) was used. Balance of four decimal places AND for weighing chemicals. FT-IR PerkinElmer machine spectrum RX1 model made in US. Scanning electron microscope (SEM, model VEGA-TESCAN-LMU) was employed to evaluate the microstructure of the material.

Metallurgy research center

Synthesis of hydrogel nano-composite Gx-el-P (AA-eo-AAm)/Fe_3O_4: Before the graft polymerization reaction, 50 mg of MNP Fe_3O_4 were ultrasonic in 20 mL of deionized water for 4 h. The reaction maintained at 60 °C. 50 mg of methylene bisacryl amide (MBA) added to the reaction mixture by vigorous mixture the final step. A mixture of 25 mL acrylic acid (AA) and 1 g of acrylamide added slowly by constant shaking and the reaction continued for 3 h without any disturbance. After 3 h, the reaction vessel cooled at room temperature. Hem polymers, including polyacrylamide and polyacrylic acid, were removed from the synthesized hydrogel nano-composite using the soxhlet extraction with acetone for about 5 to 6 h. In addition, the remaining homopolymers isolated by stirring the nano-composite hydrogel composites in acetone for 24 h using a magnetic stirrer. Finally, the synthesized hydrogel nano-composite was dried and powdered in a hot air oven at 60 °C.

Solution: To prepare nickel-containing solution, $NiN_2O_8*H_2O$ metal salt was used at 955.4 g and to adjust the PH of the environment, IC acid chloride and sodium hydroxide 0.05 molar were used. First, a 1000 ppm solution of hydrated nickel salt $NiN_2O_8*H_2O$ was made as standard solution and diluted with 0.1 M nitric acid. Then the solution was prepared by deionized water using the

$N_1V_1=N_2V_2$ solution of 500, 250, 100 ppm and a 100 ppm solution was used to make the final concentrations of 10, 30, 50, 70, 100 ppm.

Determination of calibration curve: To determine the calibration curve, different concentrations of nitric hexa hydrate solution with concentrations of 10, 30, 50, 70, and 100 ppm were prepared at ambient temperature and then their absorbance read by spectrophotometer machine and the calibration curve drawn at the end.

Table 5. Adsorption values for different initial concentrations of hydrated nickel nitrate

Nickel initial conc (ppm)	0	10	30	50	70	100
Absorption	0.0	0.098	0.315	0.515	0.715	0.985

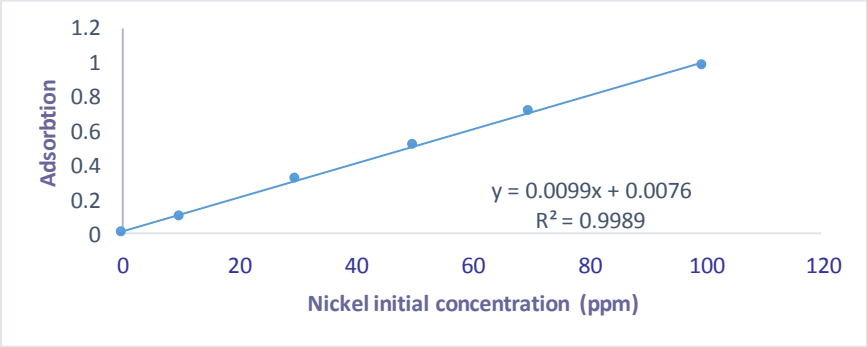

Figure 2. Adsorption calibration curve in terms of different initial concentrations of nickel nitrate

Investigation and optimization of parameters on adsorption of nickel ion (ii) on xanthan biocompatible nano-composite

Evaluation of pH effect: Add 50 mL of nickel solution (II) with 50 ppm at different pH to 0.07 g of xanthan magnetic biocompatible nano-composite. The results showed that the highest percentage of divalent nickel ion removal occurred using the xanthan magnetic biocompatible nano-composite at pH=4. Then the pH of 4 was selected as the optimum pH.

Effect of adsorbent: Add 50 mL of Ni (II) at 50 ppm with the pH of 4 to different quantities of xanthan magnetic biocompatible nano-composite in grams and at ambient temperature for one hour. Place on a magnetic stirrer at a constant speed of 300 rpm and then pass the solutions through filter paper and finally their absorption measured using the spectrophotometer.

Investigate the effect of time: 50 mL nickel (II) solution at 50 ppm concentration and pH of 4 was added to 0.1 g of bio-magnetic xanthan nano-composite adsorbent and added at ambient temperature and at different times per minute. Place the magnetic stirrer at a constant speed of 300 rpm, then pass the solutions through filter paper, and finally absorb them by spectrophotometer machine. The results

showed that the highest percentage of bivalent nickel ion removal by xanthan biocompatible nano composite adsorbent occurred within 60 min.

Investigation of effect of temperature: Add 50 mL of Ni (II) at 50 ppm and pH = 4 to 0.1 g of biosynthetic magnetic nano-composite xanthan and place on magnetic stirrer at 300 rpm for 1 h at different temperatures. The solutions removed from the filter paper and their absorbance measured using the spectrophotometer. The results showed that, the highest percentage of divalent nickel ion removal by xanthan biocompatible nano-composite adsorbent occurred at 298 K.

Effect of concentrated nickel (II) concentration: Add 50 mL of Ni (II) at 50 ppm and pH = 4 to 0.1 g of xanthan biocompatible nano-composite will be caused adsorbent at 298 K for 1 h on magnetic stirrer. At a constant speed of 300 rpm, the solutions filtered off and the absorbance measured. The results showed that the adsorption percentage decreased with increasing concentration [16-20].

Results and discussion

Effect of pH on adsorbent content: To investigate the effect of pH on nickel (II) pollutants, only acidic environments investigated because by adding the sodium hydroxide and NaOH, to the nickel solution, nickel reacted with the OH and formed insoluble precipitate $Ni(OH)_3$.

Table 6. The results of the calculations for the adsorption of Ni (II) at different pH

pH	Absorption of equilibrium solution	Equilibrium solution concentration (ppm)	Removal percentage
3	0.312	30.74	38.5
4	0.125	11.85	76.3
5	0.152	14.58	70.8
6	0.187	18.12	63.7
7	0.286	28.12	43.7

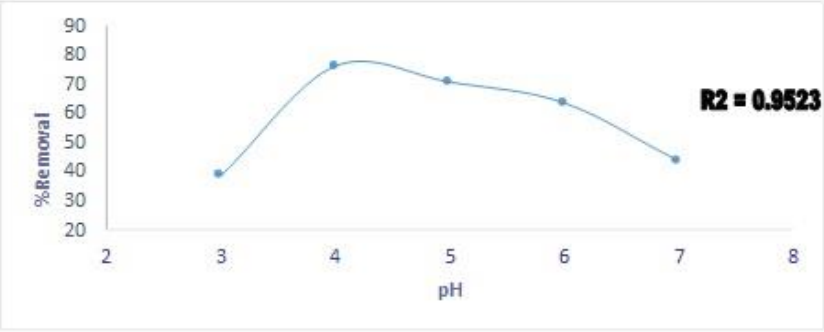

Figure 3. Influence of pH on absorption of Ni (II) ion by xanthan magnetic biocompatible nano-composite adsorbent

As seen in Figure 3, the optimum pH for the experiments was 4. By lowering the pH, the removal percentage was decreased, one of which may be due to the competition of environmental H^+ with

Ni^{+2} because by adding ric acid chloride, the number of H^+ in the medium increased, which neutralized the negative charge H^+ and reduced the tendency of Ni^{+2} to sit on the adsorbent and the absorption decreases. By adding sodium hydroxide to the nickel solution, the nickel reacted with OH and formed an insoluble precipitate $Ni(OH)_3$ causing a measurement error.

Results of investigating the effect of adsorbent on adsorption rate: It found that, the percentage of nickel ion removal calculated by different amounts of adsorbent. The graph of the effect of adsorbent on the removal of nickel ions.

Table 7. Results of the calculations for the adsorption of nickel (II) with different adsorbent amounts

Absorbent value (g)	Absorption of equilibrium solution	Equilibrium solution concentration (ppm)	Removal percentage
0.03	0.346	34.18	31.6
0.05	0.280	27.51	44.9
0.07	0.151	14.48	71.0
0.1	0.092	8.52	82.9
0.15	0.09	8.32	83.6
0.2	0.085	7.81	84.3

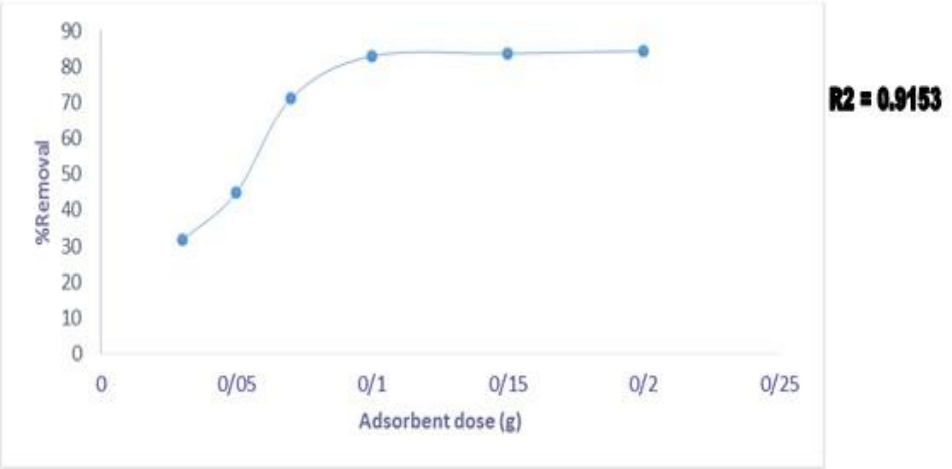

Figure 4. Influence of adsorbent on the absorption rate of nickel (II) by xanthan biocompatible nano-composite adsorbent

As can be seen in Figure 4, the optimum amount of adsorbent was 0.1 g.

Effect of contact time on adsorption rate: According to the experimental data, the adsorption capacity of nickel ion calculated using the xanthan biocompatible nano-composite adsorbent for 15, 30, 45, 60, and 90 min.

Table 8. Results of adsorption of nickel (II) ion by xanthan biocompatible nano-composite adsorbent

Time (min)	Absorption of equilibrium solution	Equilibrium solution concentration (ppm)	Removal percentage
15	0.246	24.10	51.8
30	0.191	18.52	62.9
45	0.137	13.1	73.8
60	0.089	8.20	83.6
90	0.080	7.31	85.4

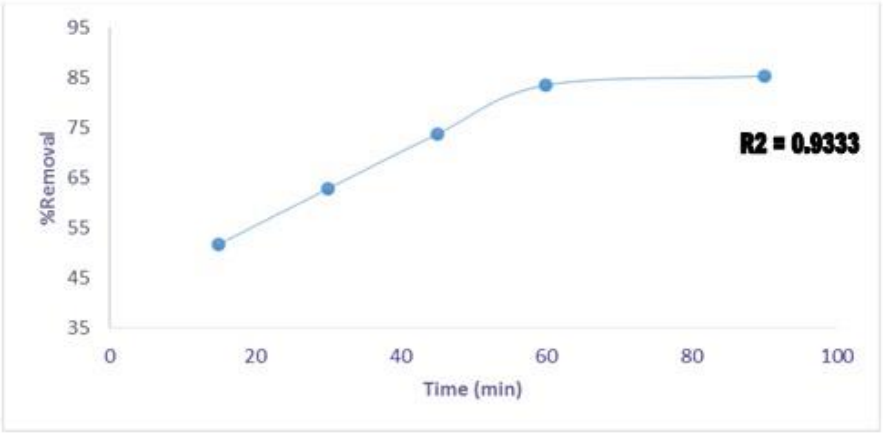

Figure 5. Influence of contact time on absorption rate of nickel (II) ion by xanthan biocompatible nano-composite adsorbent

As can be seen in Figure 5, the slope of the curve was very high in the early times because of the high concentration of nickel in the early environment and the adsorbent having many sites, meaning that the concentration gradient is at its highest. Concentration delta affected the rate of mass transfer, so ions rapidly absorbed by the adsorbent. As time passes, the concentration of the solution decreased and the concentration of the adsorbent increased.

Results of investigating of effect of temperature: According to the data obtained from the experiments, the percentage of nickel ion removal by the adsorbent measured and calculated. The graph of the effect of temperature on the removal of nickel by xanthan biocompatible nano-composite adsorbents is as follows.

Table 9. The results of the calculations for nickel (II) ion removal at different temperatures

Temperature (K)	Absorption of equilibrium solution	Equilibrium solution concentration (ppm)	Removal percentage
298	0.098	8.2	83.6
308	0.102	9.53	80.9
318	0.115	10.85	78.30
328	0.124	11.75	46.50
338	0.138	13.17	73.60
348	0.152	14.60	70.80

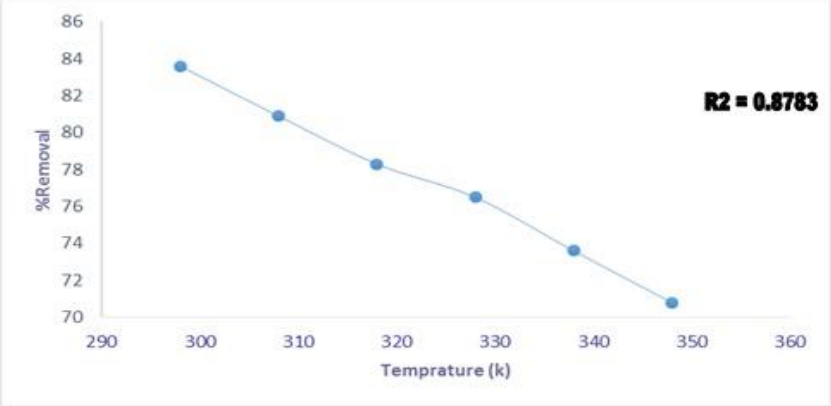

Figure 6. Effect of temperature on the removal rate of nickel ion by xanthan biocompatible nano-composite adsorbent

As can see in Figure 6, the percentage of adsorption decreased with increasing the temperature, which may indicate the physical nature of the adsorption. In fact, the increase in temperature increased the entropy, loosening the bonds between the adsorbent and the adsorbent species.

Results of the study of the effect of initial concentration on adsorption: According to the data obtained from experiments, the percentage of nickel ion removal by the adsorbent measured and calculated at different concentrations of the contaminant. It found that, by increasing the nickel concentration, the removal rate decreased. The diagram of the effect of nickel removal on xanthan biocompatible nano-composite adsorbent is as follows.

Table 10. Results of adsorption values of Ni (II) at different concentrations of nickel nitrate hexa hydrate

Initial concentration (ppm)	Absorption of equilibrium solution	Equilibrium solution concentration (ppm)	Removal percentage
10	0.01	0.24	97.6
20	0.025	1.75	91.2
30	0.042	3.47	88.4
40	0.067	6.00	85.0
50	0.091	8.42	83.1
60	0.125	11.85	80.2

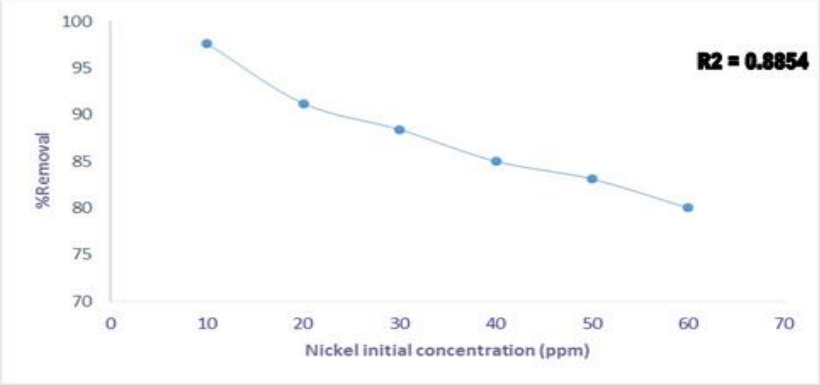

Figure 7. Effect of nickel initial concentration on nickel ion removal rate by xanthan biocompatible nano composite adsorbent

Investigation of isotherm isotherms and analysis of isotherm data: The isotherm data can be adapted to different isotherm models in order to find a suitable model to investigate the desired process. Investigation of nickel (II) adsorption isotherms on xanthan magnetic biocompatible nano-composite. The amount of adsorbed nickel on the 0.1 g adsorbent at different initial concentrations of nickel nitrate hexa hydrate calculated according to Table 11. and in the optimum condition of other variables and adsorption isotherm diagrams such as Langmuir, Freundlich and Temkin applied to the data. This study showed that, the adsorption of nickel (II) on the adsorbent follows the Freundlich adsorption isotherm.

Table 11. Effect of initial concentrations on the absorption rate of nickel (II) by xanthan biocompatible nano-composite

C_0 (mg/L^{-1})	Adsorption	C_e (mg/L^{-1})	%Removal	q_e (mg/g^{-1})	C_e/q_e	Ln C_e	Ln q_e
10	0.01	0.24	97.6	4.880	0.05	-1.43	1.58
20	0.025	1.75	91.2	9.125	0.20	0.56	2.21
30	0.042	3.47	88.4	13.265	0.26	1.24	2.58
40	0.067	6.00	85.0	17.000	0.35	1.80	2.83
50	0.091	8.42	83.1	20.790	0.40	2.13	3.03
60	0.125	11.85	80.2	24.070	0.50	2.50	3.18

Using the data in Table 12, the Langmuir equation and the C_e/q_e curve plotted in C_e and the line equation were obtained, Langmuir isotherm constants calculated. The values obtained from the dimensionless parameter of separation factor at different concentrations indicate the adsorption of divalent nickel ion onto xanthan magnetic biocompatible nano-composite was desirable.

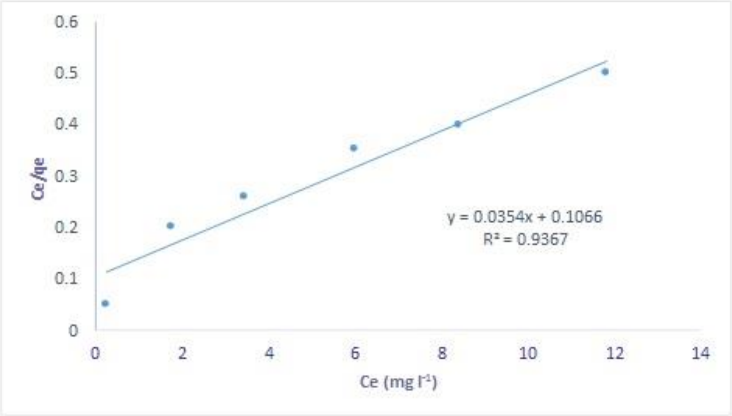

Figure 8. Langmuir adsorption isotherms for different concentrations of divalent nickel ions with different initial concentrations by xanthan biocompatible nano-composite adsorbent

Table 12. Langmuir adsorption isotherm constants

$q_{m\ (mg/g^{-1})}$	K_L (L/mg^{-1})	R^2
28.25	0.332	0.9367

Table 13. Langmuir isotherm dissociation factor values

C_0 (mg/g^{-1})	R_L
10	0.231
20	0.130
30	0.091
40	0.070
50	0.057
60	0.047

Freundlich adsorption isotherms: The values obtained from the n_f parameter, which related to the sorption intensity, indicating that the sorption process occurred physically and desirably.

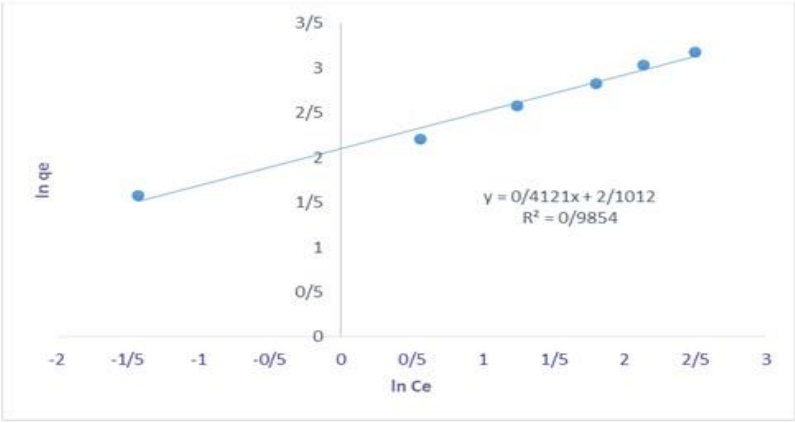

Figure 9. Freundlich isotherm for adsorption of bivalent nickel ion with different initial concentrations by xanthan biocompatible nano-composite adsorbent in optimum conditions

Table 14. Freundlich adsorption isotherm constants

n_f	K_f (mg/g^{-1})	R^2
2.42	8.176	0.9854

Investigation of the isotherm isotherm adsorption of Temkin: Using the data in Table 14, the Temkin equation and the curve drawing q_e in terms of Ln C_e and to obtain the line equation the Langmuir isotherm constants calculated.

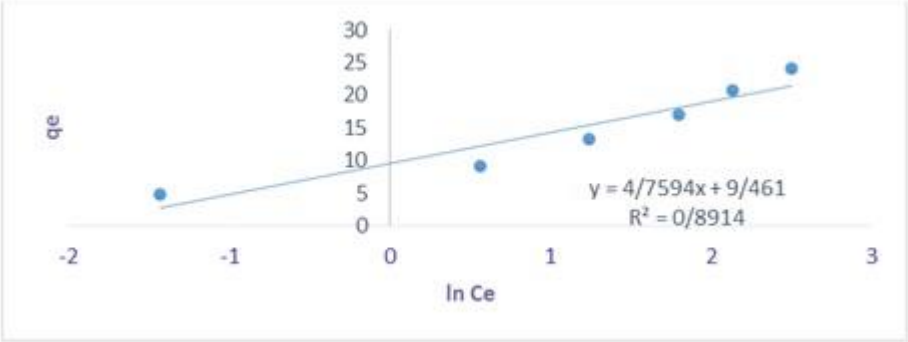

Figure 10. Temkin isotherm for adsorption of divalent nickel ion at different initial concentrations by xanthan biocompatible nano-composite adsorbent in optimum conditions

Table 15. Langmuir adsorption isotherm constants

B (J/mole^{-1})	K_T (L/mg^{-1})	R^2
4.7594	1.6530	0.8914

Adsorption kinetics: Adsorption is a multi-step process involving the transfer of the adsorbed molecules from the soluble phase to the adsorbent surface and then penetration of the soluble particles into the adsorbent pores [4]. Nowadays, researchers are looking for developing the nanotechnology and the application of nanotechnology in human life. In this regard, development of efficient, recyclable, and easily obtainable adsorbents that accurately and accurately perform the adsorption process in a short period is a part of nanotechnology studies.

Investigation of adsorption kinetics of nickel (II) on xanthan magnetic biocompatible nano composite: To investigate the kinetics of adsorption of nickel (II) on xantho magnetic biocompatible nano-composite, a series of experiments performed at different times (according to Table 16) in the concentration of 50 mg/L of nickel hexa hydrate solution and under the optimum conditions of other variables. Different kinetic models used on the experimental data to investigate the rate of adsorption process and the potential of the rate-determining step. In this regard, pseudo-first-order and pseudo-second-order kinetic models used to investigate the rate of

adsorption and calculate the corresponding constants. Correlation coefficient showed that the nickel (II) adsorption follows the pseudo-second order kinetics.

Table 16. Effect of contact time on the absorption percentage of nickel (II) by xanthan magnetic biocompatible nano-composite for the study of adsorption kinetics at pH = 4, adsorbent dose 0.1 g, temperature 298 K and 50 mg/L nickel

Time (min)	adsorption	C_e (mg/L^{-1})	%adsorption	q_t (mg/g^{-1})	q_e-q_t	Log (q_e-q_t)	t/q_t
15	0.246	24.10	51.80	12.95	11.12	1.05	1.16
30	0.191	18.52	62.90	15.74	8.33	0.92	1.9
45	0.137	13.10	73.80	18.45	5.62	0.75	2.44
60	0.089	8.2	83.60	20.90	3.17	0.50	2.87
90	0.080	7.31	85.40	21.34	2.73	0.44	4.21

Investigation of pseudo-first-order kinetic model: The pseudo-first-order kinetic equation and the log-qt linear curve (q-qt) calculated in terms of time and obtaining the line equation, pseudo-first-order kinetic model constants.

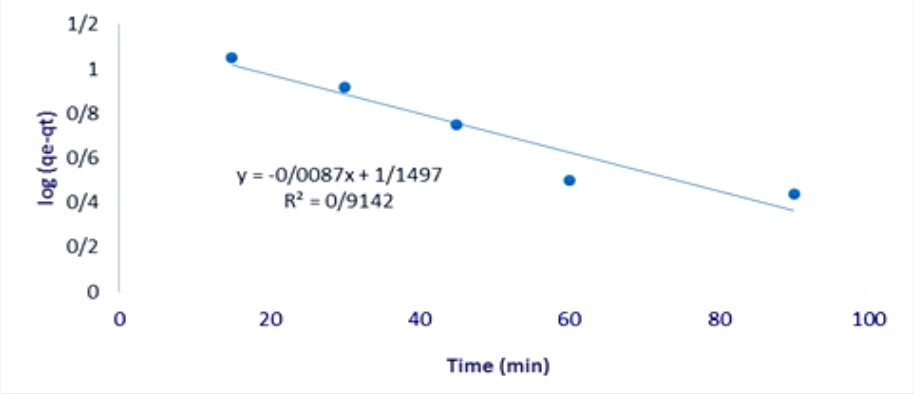

Figure 11. Quasi-first order kinetics of nickel (II) adsorption by xanthan biocompatible nano-composite adsorbent

Table 17. Pseudo-first-order kinetic parameters

q_e (mg/g^{-1})	K_1 (min^{-1})	R^2
14.11	0.02	0.9142

Investigation of pseudo-second-order kinetic model: The pseudo-second-order kinetic equation and the linear curve t computed in terms of time and obtaining the equation of the line, pseudo-second-order kinetic model constants.

Table 18. Pseudo-second-order kinetic parameters

q_e (mg/g^{-1})	K_2	R^2
25.31	0.0025	0.9944

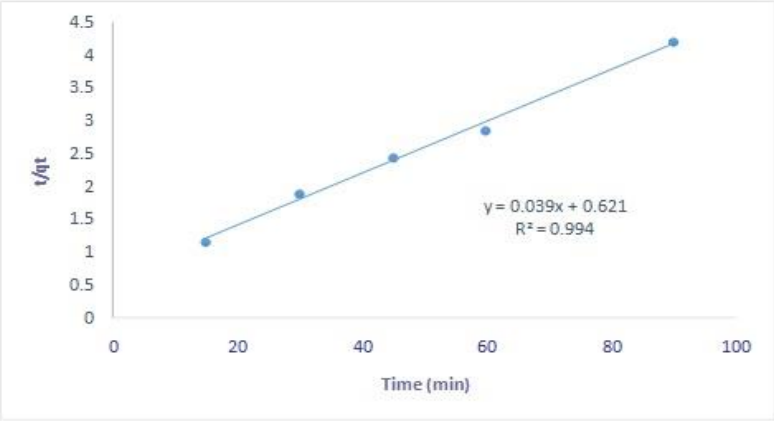

Figure 12. Pseudo-second-order kinetics of nickel (II) adsorption by xanthan biocompatible nano-composite adsorbent (error less than 2%)

Thermodynamic of adsorption

Calculation of thermodynamic variables: Using the data obtained the equilibrium constants calculated at different temperatures. Then using the equations and drawing the linear curve in terms of 1/T. Obtaining the line equation of the thermodynamic variables at different temperatures we can say: the negativity of the Gibbs standard free energy changes implies that the adsorption process is spontaneous. It should note, furthermore, that the negativity of the standard enthalpy changes is a sign of the warming of the adsorption process, also, the positivity of the standard entropy changes of the system indicates an irregular increase in the solid phase of the solid-solution adsorption process. In other words, the positivity of the standard entropy changes of the system indicates an increase in the adsorbate disorder in the contaminant adsorption process compared to the initial state prior to the adsorption process, which may suggest that the change and increase in the adsorbent structure occurred during the adsorption process.

Table 19. Equilibrium constant values for the adsorption of nickel (II) ion on xanthan biocompatible nano-composite adsorbent

T (K)	C_e (mg/L^{-1})	K_d (ml/g^{-1})	LnK_d	1/T (K^{-1})
298	8.2	418	6.03	0.0033
308	9.53	404.70	6	0.0032
318	10.85	391.50	5.97	0.0031
328	11.75	382.50	5.95	0.003
338	13.17	368.30	5.91	0.0029
348	14.60	354	5.87	0.0028

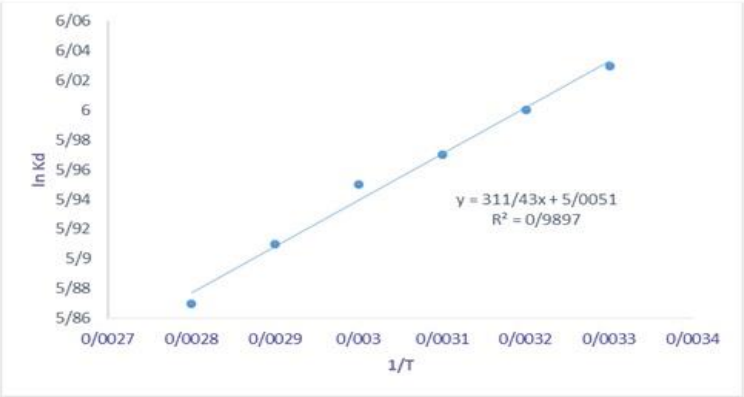

Figure 13. Vant Hoff graph for extraction of thermodynamic parameters of Ni (II) adsorption by xanthan biocompatible nano-composite adsorbent

Table 20. Thermodynamic parameters of nickel (II) absorption by xanthan magnetic biocompatible nano composite

T (K)	ΔG^0 (KJ/mole^{-1})	H^0 (KJ/mole^{-1})Δ	S^0 (KJ/mole^{-1})Δ
298	-14.94		
308	-15.36		
318	-15.78	-2.59	0.0416
328	-16/22		
338	-16.60		
348	-16.98		

Conclusions

Kinetic studies showed that the adsorption of nickel (II) on xanthan magnetic biocompatible nano-composite followed a pseudo-second-order kinetics. By increasing the concentration of the solution containing divalent nickel ions, the rate of absorption per unit mass of the adsorbent decreased. Increasing the temperature reduced the adsorption process, so the adsorption process can consider as an exothermic process. The negative Gibbs standard free energy indicated the spontaneous absorption process. The negativity of the standard enthalpy changes of the reaction revealed that the process was exothermic in the adsorption system. In addition, the positive standard entropy changes of the system indicated an increase in irregularities in the solid-soluble joint. According to the results of the absorption isotherms, the Freundlich adsorption isotherm equation had a higher and better correlation coefficient compared with that of the other adsorption isotherm equations. By calculating the n_f values, it was observed that the adsorption occurred optimally and physically.

Conflict of Interest

We have no conflicts of interest to disclose.

References

[1] Bozorgian A., Arab Aboosadi Z., Mohammadi A., Honarvar B., Azimi A. *Prog. Chem. Biochem. Res.,* 2020, **3**:31

[2] Godino-Salido M.L., Santiago-Medina A., Arranz-Mascarós P., López-Garzón, R., Gutiérrez-Valero M.D., Melguizo M., López-Garzón F.J. *Chem. Eng. Sci.*, 2014, **114**:94

[3] Kaşgöz H., Durmuş A., Kaşgöz A. *Polym. Adv. Technol.,* 2008, **19**:213

[4] Marandi G.B., Kermani Z.P., Kurdtabar M. *Sci. Technol.,* 2013, **26**:73

[5] Bozorgian A., Arab Aboosadi Z., Mohammadi A., Honarvar B., Azimi A. *Eurasian Chem. Commun.,* 2020, **2**:420

[6] Bagheri Marandi G., Hosseinzadeh H. *Polym. Polym. Compos.,* 2007, **15**:395

[7] Cohen J.C., Boerwinkle E., Mosley Jr T.H., Hobbs H. *New Eng. J. Med.,* 2006, **354**:1264

[8] Vijayaraghavan K., Padmesh T.V.N., Palanivelu K., Velan M. *J. hazard. Mater.,* 2006, **133**:304

[9] Liao B., Sun W.Y., Guo N., Ding S.L., Su S.J. *Coll. Surfaces A: Physicochem. Eng. Aspect.,* 2016, **501**:32

[10] Samimi A, Kavousi K., Zarinabadi S., Bozorgian A. *Prog. Chem. Biochem. Res.,* 2020, **3**:7

[11] Henderson A.P., Seetohul L.N., Dean A.K, Russell P., Prunean S., Zulfigur A. *Langmuir,* 2009, **25**:931

[12] Samimi A., Zarinabadi S., Shahbazi Kootenaei A.H., Azimi A., Mirzaei M. *South Afr. J. Chem. Eng.,* 2020, **31**:44

[13] Zhang Y., Wei X., Ya Z. *Chin. J. Chem.,* 2010, **28**:2274

[14] Liu G., Hong R.Y., Guo L., Liu G.H., Feng B., Li Y.G. *Coll. Surfaces A: Physicochem. Eng. Aspect.,* 2011, **380**:327

[15] Mashhadizadeh J., Bozorgian A., Azimi A. *Eurasian Chem. Commun.,* 2020, **2**:536

[16] Bozorgian A. *J. Basic Appl. Sci. Res.*, 2012, **2**:12923

[17] Lu J., Jiao X., Chen D., Li W. *J. Phys. Chem. C,* 2009, **113**:4012

[18] Luo X., Liu S., Zhou J., Zhang L. *J. Mater. Chem.,* 2009, **19**:3538

[19] Dresco P.A., Zaitsev V.S., Gambino R.J., Chu B. *Langmuir,* 1999, **15**:1945

[20] Samimi A., Zarinabadi S., Shahbazi Kootenaei A., Azimi A., Mirzaei M. *Eurasian Chem. Commun.,* 2020, **2**:150

How to cite this manuscript: Alireza Bozorgian*, Soroush Zarinabadi, Amir Samimi, Preparation of Xanthan Magnetic Biocompatible Nano-Composite for Removal of Ni^2+ from Aqueous Solution. Chemical Methodologies 4(4), 2020, 477-493. DOI:10.33945/SAMI/CHEMM.2020.4.9.